

PREDICTION OF POTENTIAL SARS-CoV-2 INHIBITOR: A COMPUTATIONAL APPROACH

AMAKU JAMES FRIDAY^{1*}, IGWE K. K² AND BUHARI MAGAJI³

¹Department of Chemistry, Michael Okpara University of Agriculture, Umudike

²Department of Veterinary Physiology, Pharmacology and Biochemistry, Michael Okpara University of Agriculture, Umudike, Nigeria

³Department of Chemistry, Faculty of Science, Gombe State University.

Corresponding Author: amakufj2006@gmail.com

ABSTRACT

The recent global fight against the spread of novel coronavirus has not been successful. This has resulted in public health emergencies across the world. Meanwhile, no effective drug or vaccine has been reported. Hence, maximum effort from stakeholders at various scales must be invoked. This study used Computer-Aided Drug Design (CADD) based approach to identify the drug-like compounds with possible capacity to inhibit SARS-CoV-2. Online tools (ZINC pharmer) was used to search for drug-like compounds, followed by molecular docking of the predicted hit compounds. The five-best ligand-receptor complex was selected based on the S-score of the predicted compounds that are higher than the reference inhibitor (chloroquine). After evaluating the binding energies, five compounds namely ZINC72170473, ZINC89801760, ZINC72435450, ZINC07987472 and ZINC63855480 were noticed to have -6.9 kcal/mol, -6.8 kcal/mol, -6.6 kcal/mol, -6.5 kcal/mol, and -6.5 kcal/mol docking score respectively. These docking scores were higher than that of chloroquine (-4.9 kcal/mol). The pharmacokinetics and drug-likeness of the lead molecule (ZINC72170473) were assessed by making use of Swiss ADME a free web tool. The result revealed that the oral bioavailability of the lead molecule was fine. Its solubility was also moderate for all class considered. The toxicity prediction on the ProTox-II webservice revealed that ZINC72170473 has an LD50 value of 600 mg/kg and belong to toxicity class 4. The quantum mechanical calculations also showed that the lead molecule (ZINC72170473) demonstrated better global reactive than the reference molecule (chloroquine). Hence, ZINC72170473 have shown drug-like characteristic and may have the capacity to inhibit the function of some essential protein(s) that are key to the viral life cycle if given a trial.

Keywords: SARS-CoV-2, Virtual Screening, Chloroquine, Molecular Docking

INTRODUCTION

The outbreak of a novel severe acute respiratory infection n(SARI) in December 2019, was observed to spread from Wuhan to other parts of China (Q. Li et al., 2020). The novel coronavirus (SARS-CoV-2 or COVID-19) is known to spread very fast,

although the report revealed that is too heavy to be airborne. It can be contracted from contact, aerosol, fomite or droplet of infected persons; besides this, the faecal-oral route is also a possible path. The novel emerged SARS-CoV-2 is classified into subgenus Sarbecovirus of the Betacoronavirus genus and it is associated

with high mortality (Zhao et al., 2020). Meanwhile, the outcome of SARS-CoV-2 genomic sequence revealed 96% identity to the bat-coronavirus and 79.6% sequence identity to SARS-CoV (Zhao et al., 2020). The devastating impact of SARS-CoV-2 was observed on its ability to binds to angiotensin-converting enzyme 2 (ACE2) receptor with 10–20 folds higher affinity than SARS-CoV (Xu et al., 2020). To date, no drugs or vaccines have been approved for the treatment of COVID-19. As at 25th April 2020, more than 3,140,000 persons have been infected out of which 948,000 patients were reported to have recovered and 218,000 death were recorded globally (https://en.wikipedia.org/wiki/Coronavirus_disease_2019).

In a bid to stop the spread SARS-CoV-2, the search for effective novel drug and vaccine have received immense global attention. On the contrary, no drugs or vaccines have demonstrated a sufficient capacity to stop the spread of COVID-19. Meanwhile, several clinical trials are in progress. It is worth mentioning that some existing drugs designed for other health challenges have shown promising impact in the fight against SARS-CoV-2. Meanwhile, drugs such as lopinavir, ritonavir, azithromycin, chloroquine and hydroxychloroquine were used in preliminary clinical studies, among which hydroxychloroquine was selected and currently employed in combination with other antibiotics as a preliminary treatment regimen for SARS-CoV-2 (Touret & de Lamballerie, 2020). This therapeutic approach is termed drug repurposing or repositioning and is effective in cubing the spread of novel diseases caused by infectious agents.

This is owing to the fact that the development of novel small-molecule therapeutics (drugs) could take between 10 to 15 years. Hence, it will be wise and beneficial to identify and reposition an existing well-characterized small-molecules (approved drugs) for use in combating the novel virus (Smith, 2020). Limitation attributed to the used of chloroquine can be trace to the dosage used for the treatment SARS-CoV-2. In addition to this, it is also necessary to determine if the benefit of chloroquine therapy depends on the age class, the clinical presentation or the stage of the disease (Dowall et al., 2015).

In other to bypass these challenges with chloroquine, computer-aided drug design (CADD) can be used to design of SARS-CoV-2-inhibitor with similar pharmacophoric features with chloroquine within a short period. This can be achieved systematically via the high throughput virtual screening of the pharmacophoric features of an existing drug that was designed for a different ailment on any available database (such as online ZINC database) to identify small-molecule with the capacity to inhibit the novel diseases (Cele, Ramesh, & Soliman, 2016; Kumalo & Soliman, 2016). This technique has demonstrated an effective potential to combat novel diseases caused by infectious agents that spread rapidly (Ashburn & Thor, 2004; Chopra & Samudrala, 2016; J. Li et al., 2016) Hence, we aim to reposition clinically approved drugs (chloroquine), designed to treat malaria patient for a Ligand-based virtual screening stemmed with molecular docking studies for the search of small molecules with the probable capacity to inhibit the spread of COVID-19.

MATERIALS AND METHODS

Pharmacophore Generation

The SMILE format of chloroquine was retrieved from the drug bank online platform. The UCSF Chimera interface was used to convert the SMILE format of chloroquine into its 3D model prior to submission to ZINCPharmer with distinct pharmacophoric features (see Table.1) (Koes & Camacho, 2012; Morris et al., 1998; Pettersen et al., 2004).

Structure-based Virtual Screening

To have obtained the best molecular interactions between biological target and inhibitors, it is imperative to establish robust steric and electronic characteristics of pharmacophore that is needed to initiate biological function (Haider et al., 2020). An online application “ZINC-pharmer” (<http://zincpharmer.csb.pitt.edu/pharmer.html>) was used for structure-based virtual screening of drug-like compounds having similar pharmacophoric with on the ZINC database. This type of screening is important for the identification of appropriate inhibitors with enhanced potential. The model molecule (chloroquine) was added to ZINCPharmer with distinct criteria (molecular weight of <500 Da, hydrogen bond donors <5, hydrogen bond acceptors <10 and rotatable bonds <6), to screen the ZINC database for the potential 5Y6N inhibitors (Koes & Camacho, 2012; Morris et al., 1998; Pettersen et al., 2004). Based on the generated pharmacophore features of chloroquine, the ZINC database was screened to obtain drug-like compounds with similar pharmacophoric features as exhibited by chloroquine.

Ligand Preparation

The 2D conformation of the small molecules (inhibitors) retrieved from the ZINC database was optimized using the MMF94 force field on Avogadro interface (Hanwell et al., 2012). Prior to the molecular docking step, the optimized 3D structures of the acquired ligands were processed by making use of the dock-prep tools on the UCSF Chimera interface.

Receptor Preparation

The complexed crystalized structure of COVID-19 was retrieved from the Protein Data Bank with ID 5r7y. The structure COVID-19 was a distinct single chains bounded to. The preparation of the biological target (receptor) acquired from the protein data bank was executed on the UCSF Chimera interface (Pettersen et al., 2004).

Molecular Docking

To further evaluate the drugable capacity of all the retrieved compounds, molecular docking assay was performed on all the hits obtained from the ZINC database to predict their binding conformation and affinity within the active site region of 5r7y. Ligand-receptor docking was achieved by making use of the AutoDockVina software (Morris et al., 1998). The grid box that defines the binding active site region of 5r7y protein was estimated from the AutoDock Vina functionality on UCSF Chimera (Pettersen et al., 2004). The grid box size and centre coordinates for the protein were x (9.84876, 10.1046), y (-1.58503, 7.31927) and z (23.884, 9.3706) respectively. The compound with higher binding affinity than the reference inhibitor

(chloroquine) is considered for further analysis. Quantum chemical calculations and the *In silico* prediction of pharmacokinetic properties of the best hit were determined

Validation and ADMET Analysis of Hits Compounds

For further evaluation of ADMET properties for the best inhibitors (ZINC72170473), the online SwissADME tool was employed (Monteiro, Scotti, & Scotti, 2019). This tool was also used to establish the drug-like characteristic of ZINC72170473, from which the potential and effectiveness of this compound were established.

Quantum Chemical Calculations

The quantum chemical calculations were carried out on Gaussian 09 equipped with Gaussview 5.0 software package (Gaussian09, 2009). This was achieved by making use of Becke–Lee Yang–Parr functional (B3LYP) method with 6-311++G (d, p) basis sets (Becke, 2005). The structure of the small molecules was optimized before theoretical analysis. Electronic transitions in the UV-Vis spectral region were calculated by time-dependent (TD) DFT method with B3LYP level and 6-311++G (d, p) basis set. The frontier molecular orbitals energies were also assessed and used to estimate reactivity descriptors such as Electronegativity (χ), hardness (η), softness (S) and electrophilicity index. The energy gap (ΔE) was determined by the energy difference between LUMO and HOMO (Koopmans, 1934). Absolute electronegativity (χ), absolute hardness (η) and electrophilicity index (ω) of ZINC72170473 were also

estimated. According to Koopmans' theorem, HOMO and LUMO orbital energies are used to evaluate the ionization potential ($IP \approx -E_{HOMO}$) and electron affinity ($EA \approx -E_{LUMO}$). Meanwhile, the electronegativity (χ) can be obtained from the average of the sum of ionization potential (IP) and electron affinity (EA) ($(\chi) = \frac{IP+EA}{2}$). The hardness ($(\eta) = \frac{IP-EA}{2}$) of a molecule is related to the gap between the HOMO and LUMO orbitals, however, the larger the HOMO-LUMO energy gap the harder the molecule (Pandey, Muthu, & Gowda, 2017; Yang & Parr, 1985). In the same trend, the global softness of ZINC72170473 is determined from the inverse of global hardness ($S) = \frac{1}{\eta}$. The chemical potential of ZINC72170473 was assessed from the average of electron affinity in combination with ionization energy ($\mu) = -\frac{IP-EA}{2}$. Meanwhile the electrophilicity index (ω) of ZINC08131939 was estimated from chemical potential (μ) and chemical hardness (η) using the relationship ($(\omega) = \frac{\mu^2}{2\eta}$).

RESULTS

Since the outbreak of SARS-CoV-2 in the city Wuhan China, extensive effort has been put to the search of a therapeutic vaccine with the capacity to efficiently combat this pathogen. Meanwhile, imperative to find a cost-effective antiviral drug/vaccine that can stop the spread of controls SARS-CoV-2. Own to the fact that it takes time to design, develop and approve a drug for a specific application, it will be necessary to repurpose or reposition an existing drug for clinical trials against the

spread of SARS-CoV-2. Hence, repositioning any drug with antiviral activity will be a wise step. Taking advantage of the aforementioned drug discovery technique, the present study mainly focused on repositioning chloroquine for a pharmacophore-based virtual database screening before molecular docking and drug-likeness profiling of the lead molecule as SARS-CoV-2 inhibitor.

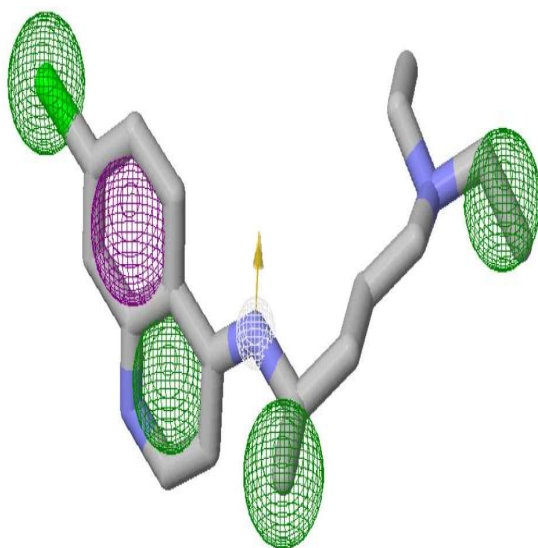


Figure 1: The 3D image of chloroquine showing the pharmacophoric signals on the ZINC Pharmer online Platform

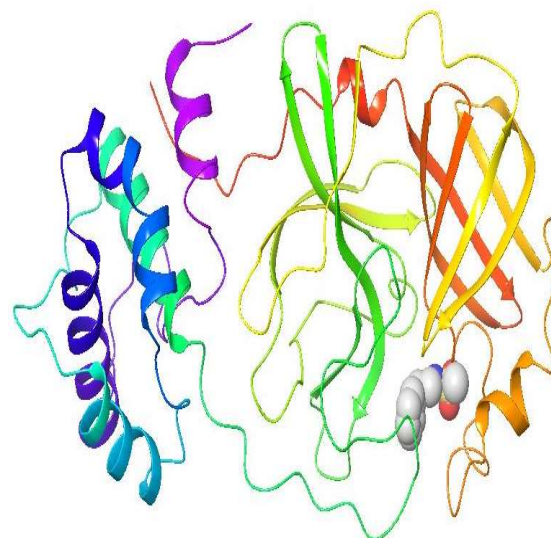


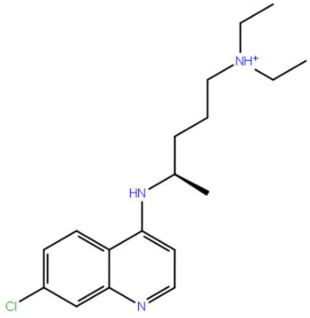
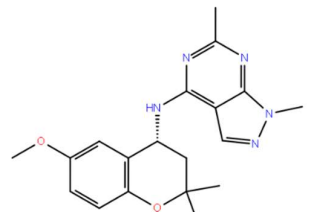
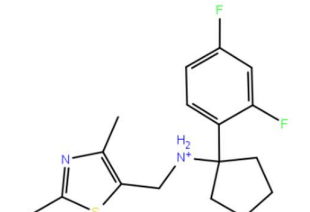
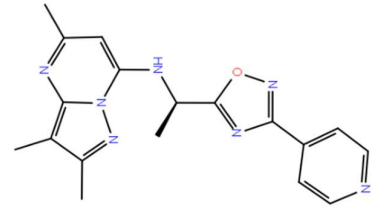
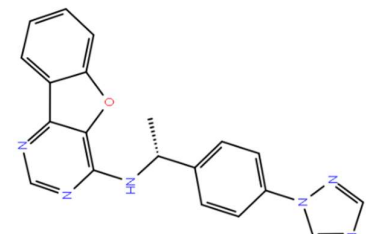
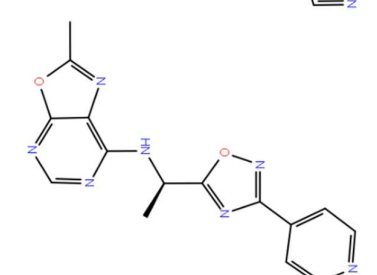
Figure 2: The 3d structure of 5r7y.

Table 1: The dimensions of the pharmacophoric features of chloroquine on ZINCpharmer Platform.

Pharmacophore Class	X	y	Z	Radius
Aromatic	3.14	0.41	0.17	1.10
Hydrophobic	0.86	-3.58	1.42	1.00
Hydrophobic	-2.19	-1.52	-0.87	1.00
Hydrogen donor	0.10	0-1.36	0.73	0.50
Hydrophobic	-5.46	2.46	0.42	1.00
Hydrophobic	6.49	0.94	-0.27	1.00

The pharmacophoric features (aromatic, hydrophobic and hydrogen donor) of chloroquine and its coordinate are listed in Table 1. The 3d-pharmacophoric signals of chloroquine employed for ZINC-pharmer search is displayed in Fig.1. Fig. 2, showed the 3d structure of SARS-CoV-2 with ID 5r7y used for specific molecular docking.

Table 2: 2D representation, ZINC code and Glide score (G-Score) value calculated with respect to the related query, of the shared best 5 hits.

CODE	SCORE * ΔG (Kcal/mol)	STRUCTURE
Chloroquine	-4.9	
ZINC72170473	-6.9	
ZINC89801760	-6.8	
ZINC72435450	-6.6	
ZINC07987472	-6.5	
ZINC63855480	-6.5	

The docking pose of the five best predicted ligands compare to chloroquine and their corresponding ligand interactions within the pocket of 5r7y are shown in Figs. 3 to 8.

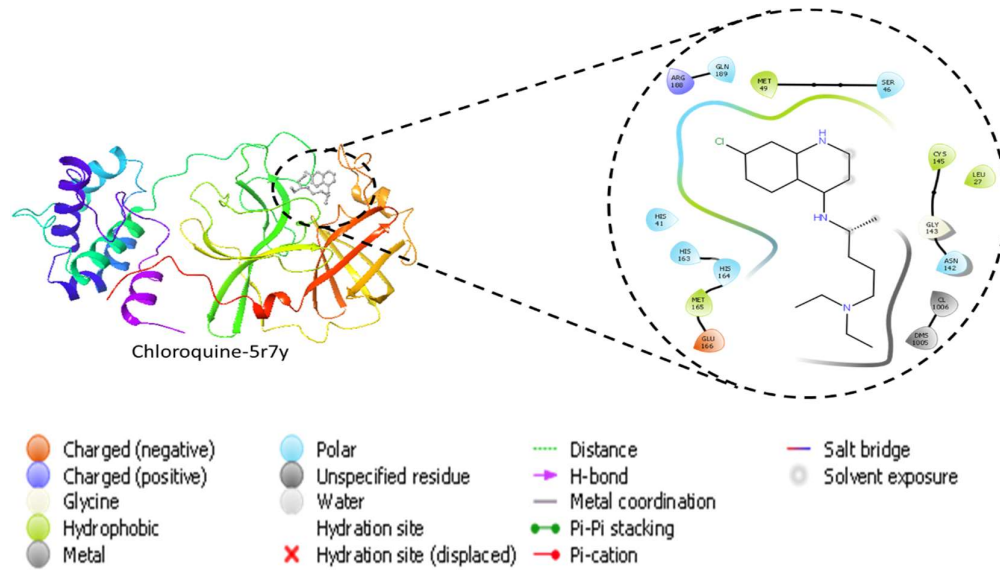


Figure 3: The 3D X-ray crystal structure of 5r7y complex with chloroquine showing also the binding site region and the residues that constitute this binding site region.

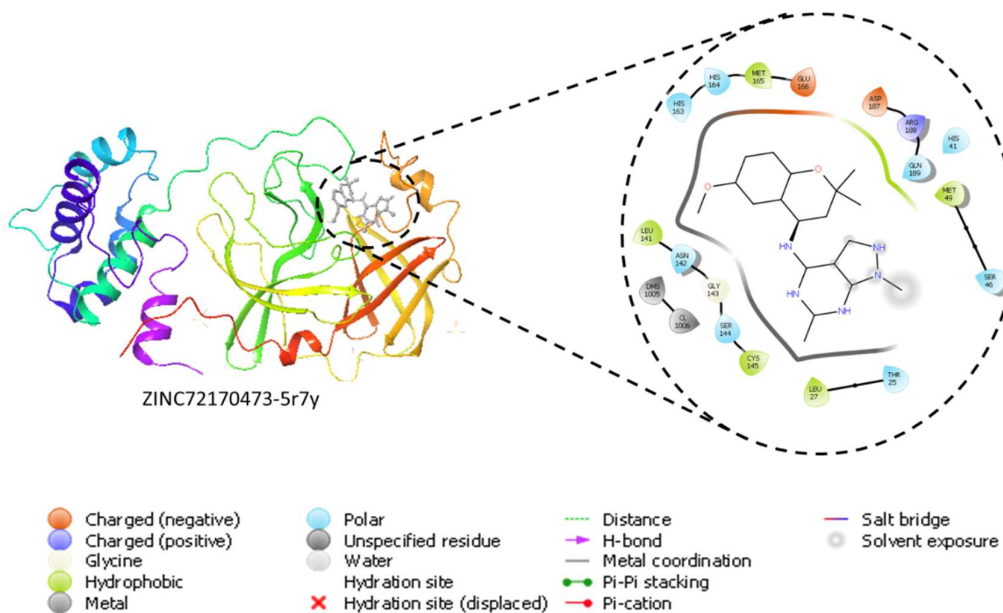


Figure 4: The 3D X-ray crystal structure of 5r7Y complex with ZINC72170473 showing also the binding site region and the residues that constitute this binding site region.

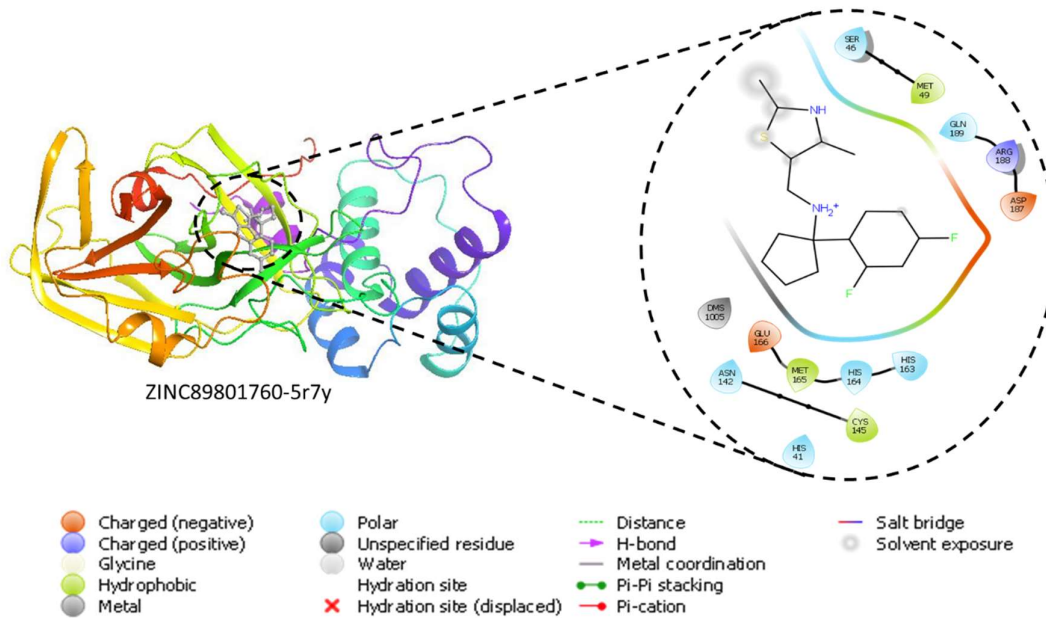


Figure 5: The 3D X-ray crystal structure of 5r7y complex with ZINC89801760 showing also the binding site region and the residues that constitute this binding site region.

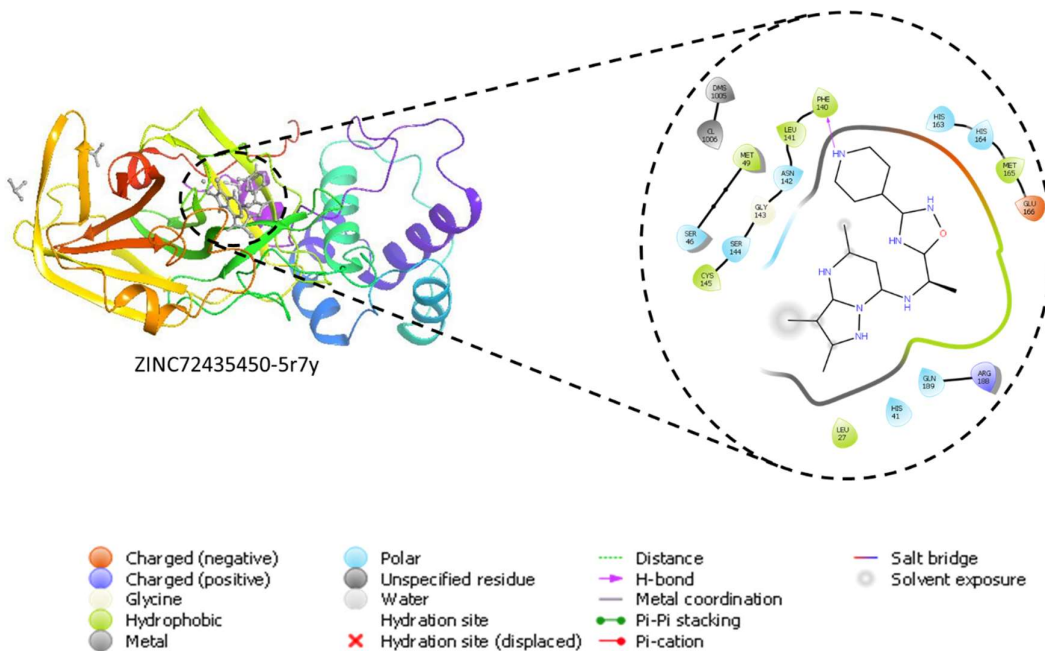


Figure 6: The 3D X-ray crystal structure of 5r7y complex with ZINC72435450 showing also the binding site region and the residues that constitute this binding site region.

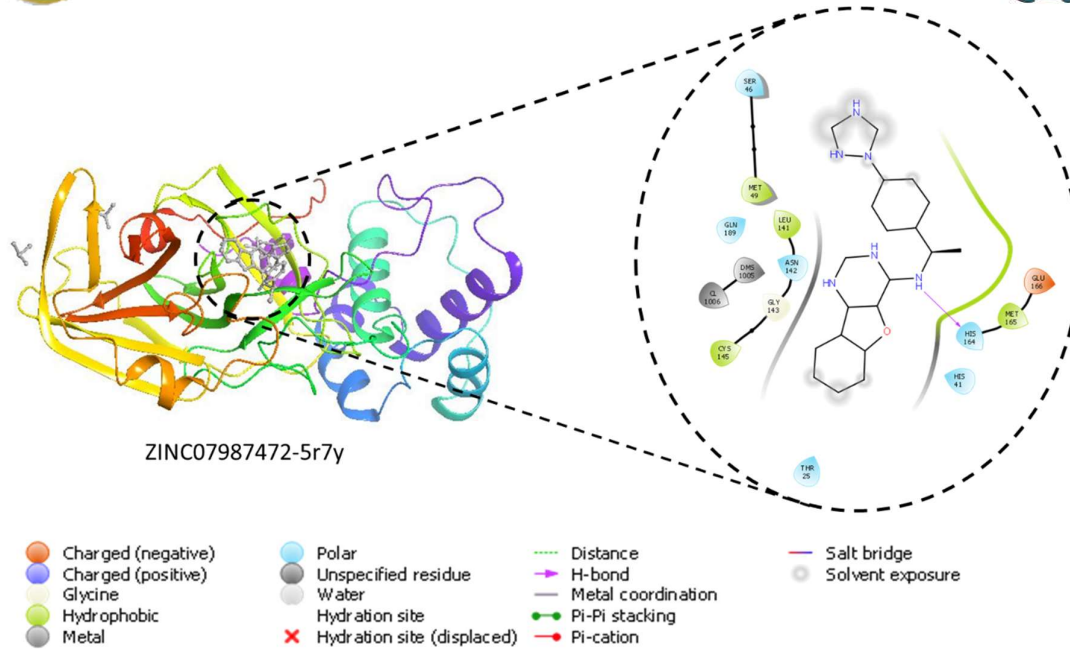


Figure 7: The 3D X-ray crystal structure of 5r7y complex with ZINC07987472 showing also the binding site region and the residues that constitute this binding site region.

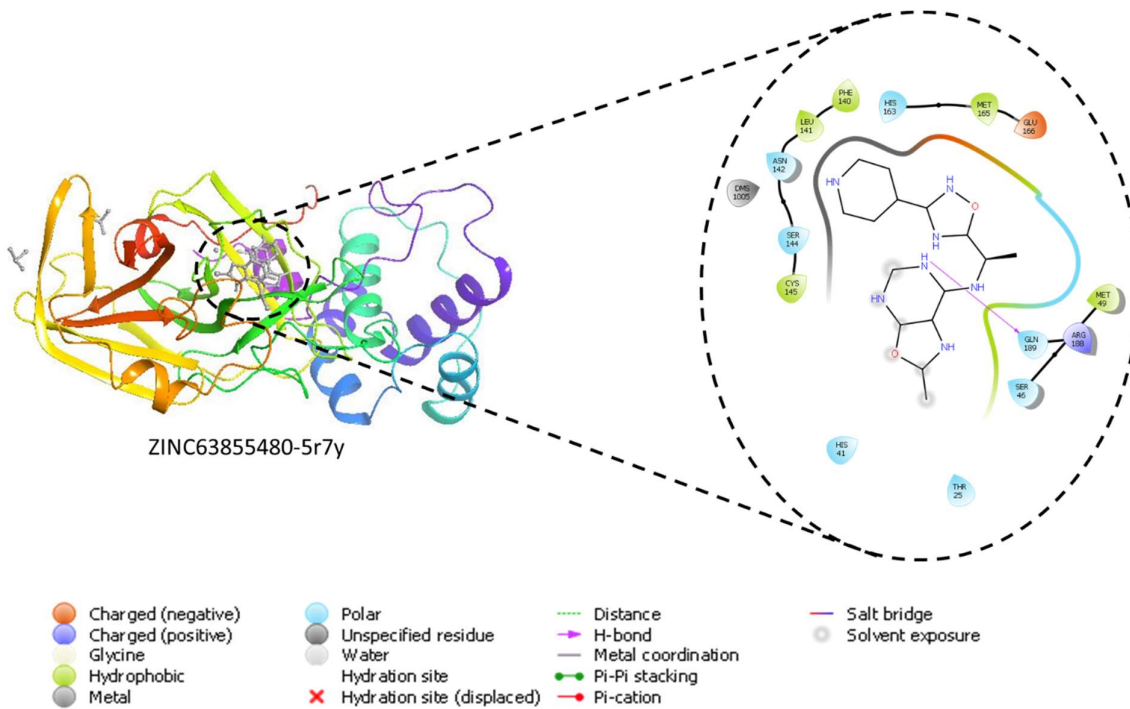


Figure 8: The 3D X-ray crystal structure of 5r7y complex with ZINC63855480 showing also the binding site region and the residues that constitute this binding site region.

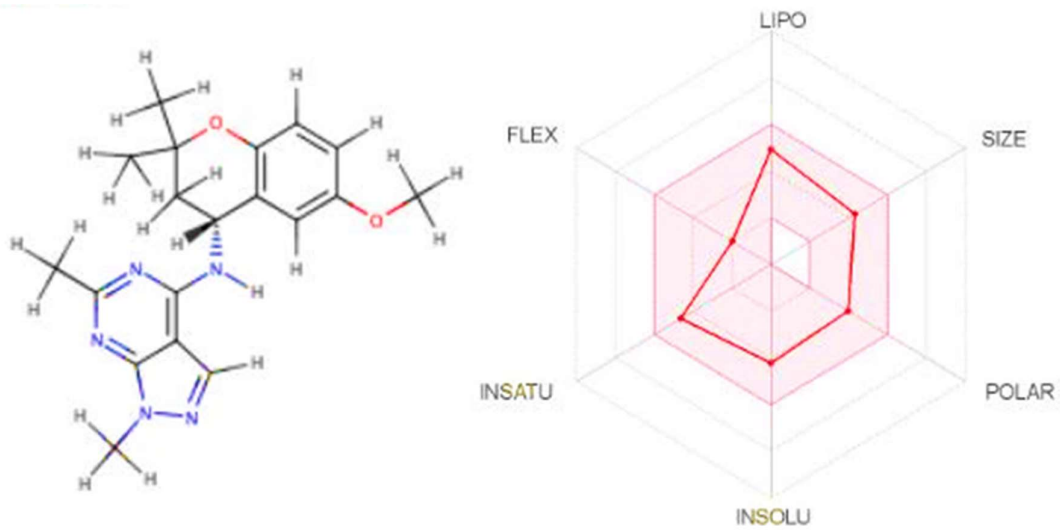


Figure 9: The bioavailability radar of ZINC72170473 using Swiss ADME predictor.

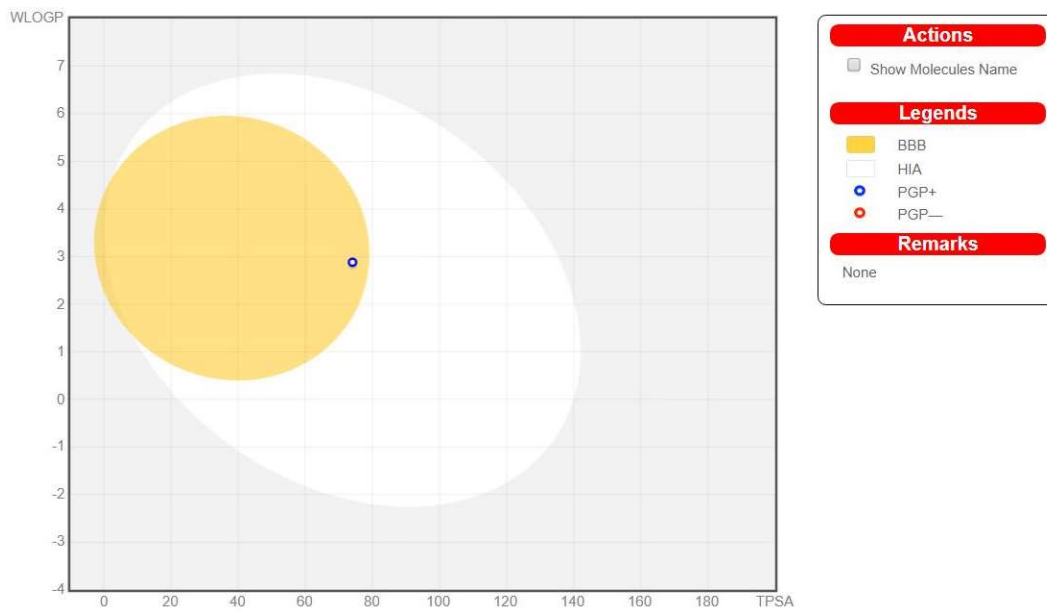


Figure 10: Molecule falling in egg's yolk prediction of ZINC72170473.

Table 3: Water solubility of ZINC72170473

Log S (ESOL)		-4.23
	Solubility	2.10e ⁻² mg ml ⁻¹ ; 5.95e ⁻⁵ mol ml ⁻¹
	Class	Moderately soluble
Log S (Ali)		-4.34
	Solubility	1.60e ⁻² mg ml ⁻¹ ; 4.52e ⁻⁵ mol ml ⁻¹
	Class	Moderately soluble
Log S (SILICOS-IT)		-5.87
	Solubility	4.73e ⁻² mgml ⁻¹ ; 1.34e ⁻⁵ mol ml ⁻¹
	Class	Moderately soluble

Table 4: Pharmacokinetics of ZINC72170473

GI adsorption	High
BBB permeant	Yes
P-gp substrate	Yes
CYP 1A2	Yes
CYP2C19	No
CYP2C9	Yes
CYP2D6	Yes
CYP3A4	Yes

Log Kp (skin permeation) -6.24 cm s⁻¹

Table 5: Drug likeness of ZINC72170473

Lipinski	Yes, 0 violation
Ghose	Yes
Veber	Yes
Egan	Yes
Muegge	No
Bioavailability score	0.55

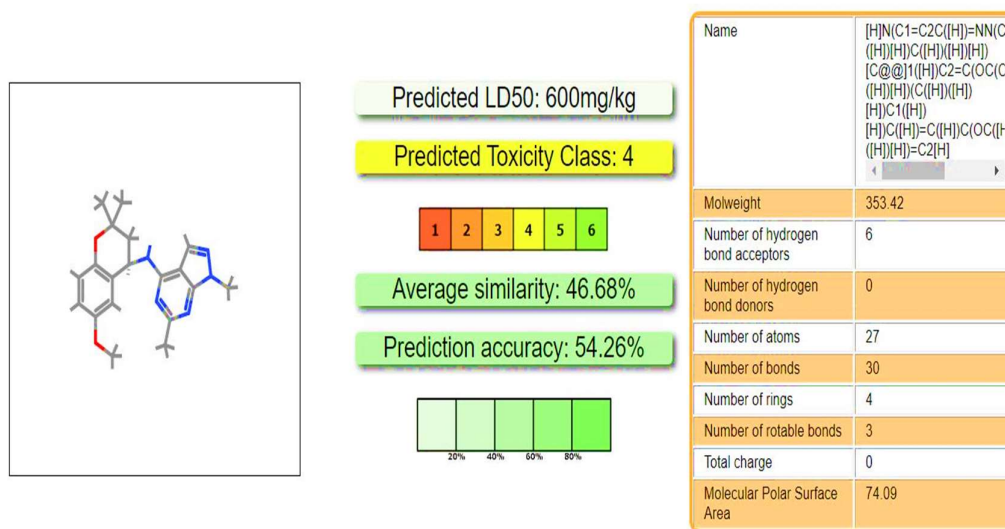


Figure 11: The oral toxicity prediction of ZINC72170473

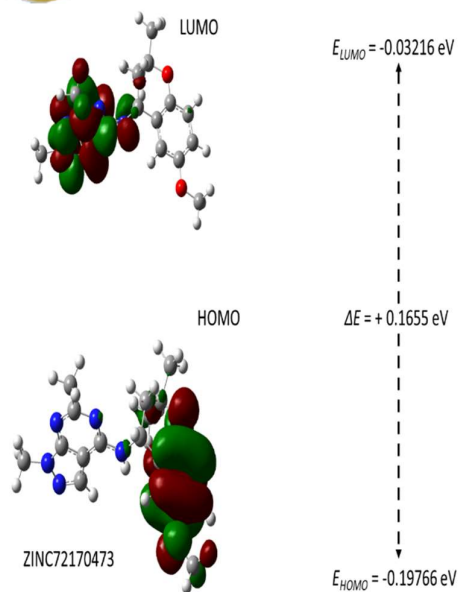


Figure 12: HOMO, LUMO orbitals at the B3LYP/6-311++G (d, p) basis set for ZINC72170473.

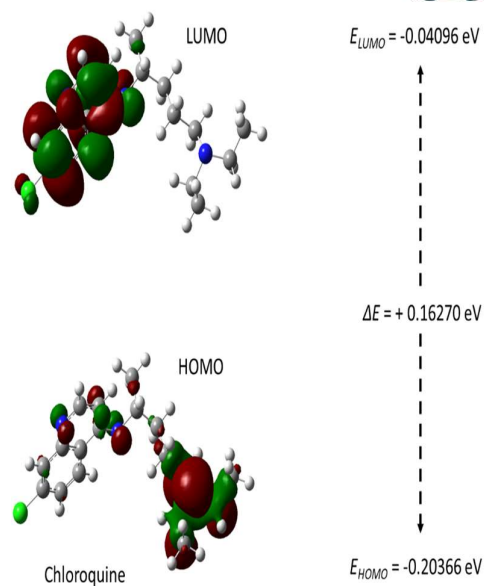


Figure 13: HOMO, LUMO orbitals at the B3LYP/6-311++G (d, p) basis set for chloroquine.

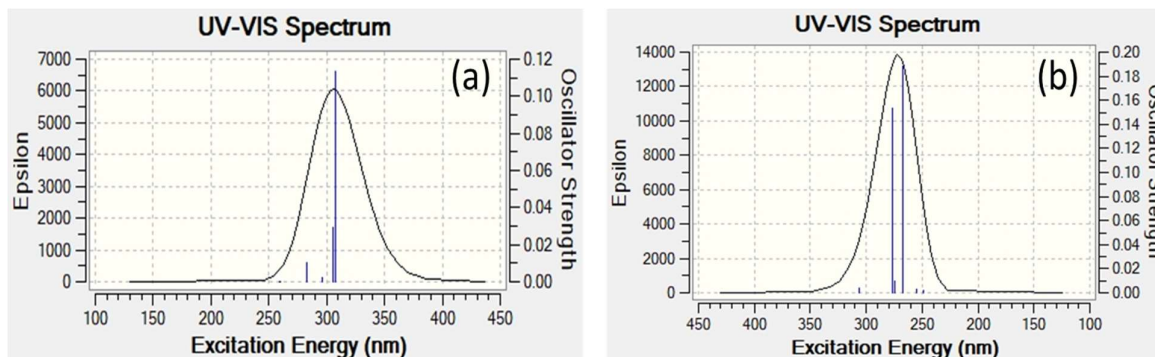


Figure 14: The predicted UV-VIS spectra of (a) chloroquine and (b) ZINC84071344

Table 6: HOMO-LUMO energies and calculated global reactivity parameters of ZINC72170473 and chloroquine molecule, calculated by B3LYP/6-311++G (d,p) method

Parameters	ZINC72170473	Chloroquine
E_{HOMO} (eV)	-0.19766	-0.20366
E_{LUMO} (eV)	-0.03216	-0.04096
$(E_{LUMO}(\text{eV}) - E_{HOMO}(\text{eV}))$ (eV)	0.1655	0.16270
Electronegativity (χ)	0.11491	0.12231
Chemical hardness(η)	0.08275	0.08135
Softness(S)	12.0846	12.2926
Chemical potential (ω)	-0.08275	-0.08135
Electrophilicity index (ω)	0.04138	0.04068

DISCUSSION

Pharmacophore-based Virtual Screening and Database Preparation

In computer-aided drug design (CADD), virtual screening is an efficient and quick method to discover novel drug compounds. To achieve this, The pharmacophore model of chloroquine was retrieved from the drug bank database. The model was used to screen for small molecules with similar pharmacophoric features with chloroquine by making use of ZINCpharmer (see Fig. 1). To achieve this, virtual screening of the model (chloroquine) was performed on the ZINC database by making use of ZINCpharmer. The pharmacophore key features with four hydrophobic, one aromatic, one and one H-donor were selected to generate a pharmacophore model and screened the ZINC database containing ~250 million compounds in 3D format (see Table 1). At the end of the search, 90 out of 100 were retrieved.

Molecular Docking

Molecular docking refers to physical three dimensional (3D) structural interactions between a target (proteins, DNA, receptors, RNA, etc.) and a ligand (small molecules, proteins, peptides, etc.) to give a stable adduct. This CADD technique (docking) is primarily designed to predict conformational accuracy.(Chopra & Samudrala, 2016). The predicted eighty-five molecule obtained from the ZINCdata base were docked against 5r7y and about seventy-nine of these small molecules were noticed to have docking scores higher than the reference molecule (Chloroquine). Meanwhile, the top five drug-like compounds as shown in the energetic data

(see Table 2), were considered as auspicious candidates for further analysis. The ligand interaction with the amino acid residues within the pocket of the studied receptor (5r7y) was shown in Figs.3.to 8. This was carried out by further uploading the bound complexes onto the Schrodinger 2018 software (Maestro 11.1).

A comparison of residue interaction profiles of the potential inhibitors to that 5r7y to further assess their inhibitory prospects. The reference molecule (chloroquine) were observed to interact with fifteen amino acid residues with a binding score of -4.9 kcal/mol. Meanwhile, both ZINC63855480 and ZINC07987472 interacted with 15 and 14 similar amino acid residues respectively within the binding site of 5r7y with a binding score of -6.5. On the other hand, ZINC72435450(-6.6 kcal/mol) and ZINC89801760 (-6.8 kcal/mol) had physical interactions with 13 and 18 amino acid residues respectively. Pocket interaction analysis revealed that ZINC72170473 interacted with nineteen residues (LUE 27, THR 25, CYS 145, SER 144, GLY 143, CI 1006, DMS 1005, ASN 142, LEU 141, HIS 163, HIS 164, MET 165, GLU 166, ASP 187, ARG 188, GLN 189, HIS 41, MET 49, SER 46) within the binding sites of 5r7y with a binding affinity of -6.9 kcal/mol.

In comparison, ZINC72170473 interacted with more residues within the binding pocket than chloroquine, this might account for the poor affinity of chloroquine. Several reports suggest that the more negative the binding affinity of an inhibitor to its target, then the stronger the binding(Abdullahi, Olotu, & Soliman, 2018; Patil et al., 2010). Hence, the higher binding affinity of the lead molecules as deduced from docking score (see Table 2),

indicates that ZINC72170473 may have a better physiological implication on 5r7y than the repositioned chloroquine. The activity of the ligands within the hydrophobic pocket of the receptor (5r7y) could be as a result of intermolecular interactions such van der Waals, conventional hydrogen bonds, Pi Amide stacked and Pi alkyl interactions. Hence, ZINC72170473 can be considered as a candidate drug for in vitro studies and in vivo studies in the combat against SARS-CoV-2.

ADMET Assessment of Potential SARS-CoV-2 Inhibitors

The pharmacokinetics, drug-likeness and medicinal chemistry friendliness of ZINC72170473 were assessed by making use of Swiss ADME a free web tool. The suitable physicochemical space for oral bioavailability of ZINC72170473 is displayed in the coloured zone as shown in Fig. 9. The for oral bioavailability characteristics of ZINC72170473 were considered as flexibility, lipophilicity, saturation, size, polarity and solubility.

Boiled egg model was used to evaluates the pharmacokinetic properties of ZINC72170473 as a function of the blood-brain barrier (BBB) and passive gastrointestinal absorption (HIA) (see Fig. 10). The white and yellow (yolk) region indicates the high probability of passive absorption by the gastrointestinal tract and high probability of brain penetration respectively. Hence, the boiled egg model of ZINC72170473 shows that the molecule will have high gastrointestinal absorption and easily permeate the blood-brain barrier. As shown in the boiled egg model, ZINC72170473 is a P-glycoprotein (P-gp)

substrate, hence, the slight challenge in the excretion of ZINC72170473 will be expected.

As shown in Table 3, the solubility of ZINC72170473 was noticed to be moderate in all the major class considered for the study. This further justifies the drugable characteristic ZINC72170473. Table 4 revealed the inhibition of CYP 1A2, CYP2C9, CYP2D6 and CYP3A4 isoenzyme. However, CYP2C19 was not inhibited by ZINC72170473. This suggests the possibility of drug-drug interactions which may result in the accumulation of drug/ metabolites, hence, toxic ADME process is suspected.

The Drug likeliness of a molecule is a function of the relationship between its pharmacokinetic properties and biological activities. In this study, five parameters were used to assess the capacity of ZINC72170473 to function as a drug, Lipinski rule of five stats that the molecular weight of the compound should be less than 500 daltons, the hydrogen bond acceptor should be not more than 10, the hydrogen bond donor should be more than 5 and log P value should be not more than 5. Meanwhile, ZINC72170473 was noticed to obey Lipinski, Ghose, Egan, Verber and Muegge rules. This assessment was based on the range set values stipulated by these rules (see Table 5)

A variety of technique, such as *in silico* predictions is a modelled approach *via* which toxicity risks associated with drug usage are rationalized in the preclinical stage of drug development. In this study, toxicity risks of ZINC72170473 were predicted using the ProTox-II webserver. This revealed that ZINC72170473 has an LD50 value of 600 mg/kg and belong to toxicity class 4. The prediction was made

with a similarity index of 46.68% and accuracy of 54.26% (see Fig. 11)

Global Reactivity Descriptors

The density functional theory (DFT) approach was used to assess chemical reactivity descriptors as chemical hardness, chemical potential, polarizability and electrophilicity index of chloroquine and ZINC72170473 (see Table 6). These descriptors were calculated from the LUMO and HOMO energy values of chloroquine and ZINC72170473 (see Figs. 12 and 13). The energy gap of the lead molecule was observed to be higher than that of the reference molecule (chloroquine). A similar trend was noticed in the values of the hardness descriptors. This suggests that the lead molecule (ZINC72170473) may be more reactive than the reference molecule. The close wavelength maxima of absorption (for chloroquine and ZINC72170473), shows that the virtual screening step was effective (see Fig. 14). Hence, the lead molecule (ZINC72170473) possesses similar pharmacophoric features with chloroquine.

CONCLUSION

This study is aimed at the pharmacophore-based virtual screening of the ZINC database with the pharmacophoric features of chloroquine as a reference, molecular docking of predicted molecules and evaluation of binding interaction of the best molecule (best binding affinity) with 5r7y. Meanwhile, five compounds from the ZINC database (ZINC72170473, ZINC89801760, ZINC72435450, ZINC07987472 and ZINC63855480) showed the strong interaction against the active site of the of SARS-CoV-2.

However, ZINC72170473 demonstrated better activity and enhanced global reactivity, hence, could have potential to be utilized for the choice of a candidate against SARS-CoV-2. In the preliminary design and development of a drug against SARS-CoV-2, ZINC72170473 may be useful for in vitro and in vivo studies

REFERENCES

- Abdullahi, M., Olotu, F. A., & Soliman, M. E. (2018). Allosteric inhibition abrogates dysregulated LFA-1 activation: Structural insight into mechanisms of diminished immunologic disease. *Computational biology and chemistry*, 73, 49-56.
- Ashburn, T. T., & Thor, K. B. (2004). Drug repositioning: identifying and developing new uses for existing drugs. *Nature reviews Drug discovery*, 3(8), 673-683.
- Becke, A. D. (2005). Real-space post-Hartree-Fock correlation models. *The Journal of Chemical Physics*, 122(6), 064101.
- Cele, F. N., Ramesh, M., & Soliman, M. E. (2016). Per-residue energy decomposition pharmacophore model to enhance virtual screening in drug discovery: a study for identification of reverse transcriptase inhibitors as potential anti-HIV agents. *Drug design, development and therapy*, 10, 1365.
- Chopra, G., & Samudrala, R. (2016). Exploring polypharmacology in drug discovery and repurposing using the CANDO platform. *Current pharmaceutical design*, 22(21), 3109-3123.

- Dowall, S. D., Bosworth, A., Watson, R., Bewley, K., Taylor, I., Rayner, E., . . . Pitman, J. (2015). Chloroquine inhibited Ebola virus replication in vitro but failed to protect against infection and disease in the in vivo guinea pig model. *The Journal of general virology*, 96(Pt 12), 3484.
- Gaussian09, R. A. (2009). M.J. Frisch, G.W. Trucks, H.B. Schlegel, G.E. Scuseria, M.A. Robb, J.R. Cheeseman, J.A. Gonzalez, J.A. Pople, Gaussian 09, Revision E.01, Gaussian, Inc, Wallingford, CT, 2004. *Inc., Wallingford CT, 121*, 150-166.
- Haider, Z., Subhani, M. M., Farooq, M. A., Ishaq, M., Khalid, M., Khan, R. S. A., & Niazi, A. K. (2020). In Silico discovery of novel inhibitors against main protease (Mpro) of SARS-CoV-2 using pharmacophore and molecular docking based virtual screening from ZINC database: Preprints.
- Hanwell, M. D., Curtis, D. E., Lonie, D. C., Vandermeersch, T., Zurek, E., & Hutchison, G. R. (2012). Avogadro: an advanced semantic chemical editor, visualization, and analysis platform. *Journal of cheminformatics*, 4(1), 17.
- Koes, D. R., & Camacho, C. J. (2012). ZINCPharmer: pharmacophore search of the ZINC database. *Nucleic acids research*, 40(W1), W409-W414.
- Koopmans, T. (1934). Über die Zuordnung von Wellenfunktionen und Eigenwerten zu den einzelnen Elektronen eines Atoms. *Physica*, 1(1-6), 104-113.
- Kumalo, H., & Soliman, M. E. (2016). Per-residue energy footprints-based pharmacophore modeling as an enhanced in silico approach in drug discovery: a case study on the identification of novel β -secretase1 (BACE1) inhibitors as anti-Alzheimer agents. *Cellular and Molecular Bioengineering*, 9(1), 175-189.
- Li, J., Zheng, S., Chen, B., Butte, A. J., Swamidass, S. J., & Lu, Z. (2016). A survey of current trends in computational drug repositioning. *Briefings in bioinformatics*, 17(1), 2-12.
- Li, Q., Guan, X., Wu, P., Wang, X., Zhou, L., Tong, Y., . . . Wong, J. Y. (2020). Early transmission dynamics in Wuhan, China, of novel coronavirus-infected pneumonia. *New England Journal of Medicine*.
- Monteiro, A., Scotti, M., & Scotti, L. (2019). *Molecular docking of fructose-derived nucleoside analogs against reverse transcriptase of HIV-1*. Paper presented at the Proceedings of MOL2NET 2019, International Conference on Multidisciplinary Sciences, 5th edition.
- Morris, G. M., Goodsell, D. S., Halliday, R. S., Huey, R., Hart, W. E., Belew, R. K., & Olson, A. J. (1998). Automated docking using a Lamarckian genetic algorithm and an empirical binding free energy function. *Journal of computational chemistry*, 19(14), 1639-1662.
- Pandey, M., Muthu, S., & Gowda, N. N. (2017). Quantum mechanical and spectroscopic (FT-IR, FT-Raman, ¹H, ¹³C NMR, UV-Vis) studies,

- NBO, NLO, HOMO, LUMO and Fukui function analysis of 5-Methoxy-1H-benzo [d] imidazole-2 (3H)-thione by DFT studies. *Journal of Molecular Structure*, 1130, 511-521.
- Patil, R., Das, S., Stanley, A., Yadav, L., Sudhakar, A., & Varma, A. K. (2010). Optimized hydrophobic interactions and hydrogen bonding at the target-ligand interface leads the pathways of drug-designing. *PLoS ONE*, 5(8).
- Petterson, E. F., Goddard, T. D., Huang, C. C., Couch, G. S., Greenblatt, D. M., Meng, E. C., & Ferrin, T. E. (2004). UCSF Chimera—a visualization system for exploratory research and analysis. *Journal of computational chemistry*, 25(13), 1605-1612.
- Smith, J. C. (2020). Repurposing Therapeutics for COVID-19.
- Touret, F., & de Lamballerie, X. (2020). Of chloroquine and COVID-19. *Antiviral research*, 104762.
- Xu, Z., Peng, C., Shi, Y., Zhu, Z., Mu, K., Wang, X., & Zhu, W. (2020). Nelfinavir was predicted to be a potential inhibitor of 2019-nCov main protease by an integrative approach combining homology modelling, molecular docking and binding free energy calculation. *bioRxiv*.
- Yang, W., & Parr, R. G. (1985). Hardness, softness, and the fukui function in the electronic theory of metals and catalysis. *Proceedings of the National Academy of Sciences*, 82(20), 6723-6726.
- Zhao, S., Lin, Q., Ran, J., Musa, S. S., Yang, G., Wang, W., . . . He, D. (2020). Preliminary estimation of the basic reproduction number of novel coronavirus (2019-nCoV) in China, from 2019 to 2020: A data-driven analysis in the early phase of the outbreak. *International journal of infectious diseases*, 92, 214-217.